Magnetoexciton electroabsorption in T-shaped semiconductor quantum wires

Justino R. Madureira
Instituto de Física, Universidade Estadual de Campinas, 13083-970, CP 6165, Campinas-SP, Brazil

Marcelo Z. Maialle
Liceu Vivere, Pirassununga-SP, 13635-000, Brazil

Marcos H. Degani
Universidade São Francisco, 13251-900, Itatiba-SP, Brazil
(Received 16 April 2002; published 26 August 2002)

This work presents a calculation of the optical absorption spectra of magnetoexcitons in T-shaped semiconductor quantum wires. The calculation is performed using the semiconductor Bloch equations in the real-space and time domains. The peak and the linewidth of the fundamental exciton transition are investigated as functions of the applied magnetic and electric fields. For increasing magnetic field the exciton has its binding energy enhanced. The absorption spectra in the presence of a static electric field along the wire axis show a line broadening, an energy shift, and oscillations characteristic of the Franz-Keldysh effect. An introductory study of the effects on the absorption spectra of phase space occupation by photocreated carriers was done and we found that optical gain occurs for carrier density above $\sim 1.5\times 10^6/\mathrm{cm}$.

DOI: 10.1103/PhysRevB.66.075332 PACS number(s): 78.67.−n, 85.35.Be, 71.35.−y

The peculiar optical and electronic properties of nanometric systems with quantum-confined electronic states are promising for uses in devices. The realization of one-dimensional (1D) semiconductor nanostructures is nowadays accomplished in different ways. One is the so-called T-shaped quantum wire, formed at the intersection of two quantum wells grown on perpendicular crystallographic planes (see Fig. 1). The fundamental electronic state in the T wire, which is quantum confined in two directions and translationally invariant along one direction, lies below the fundamental quasi-2D states in the constituent quantum wells, by typically a few tens of meV. The forced proximity of the electron-hole (e-h) pair enhances the binding energy of an exciton in the wire. A magnetic field B applied perpendicularly to the plane of the arm quantum well (see Fig. 1) can be used to externally intensify this proximity and consequently to produce an energy shift of the fundamental excitonic transition. On the one hand, the magnetic field enhances the confinement in the wire causing a diamagnetic shift to higher energies of the electron and hole subbands. On the other hand, the stronger the confinement in the wire the higher the exciton binding energy yielding an opposite energy shift. The unbalance of these contributions produces the observed blueshift of the fundamental transition for increasing magnetic field.[1]

A model calculation performed by Bryant and Band[2] to simulate the experiment[1] has shown that the field modifies the soft electronic confinement causing the electron and hole wave functions to be more or less spread over the arm quantum well or over the stem quantum well. Since the former and latter quantum-well planes are, respectively, normal and parallel to the magnetic field direction, the effect is not a pure diamagnetic shift i.e., $\propto B^2$. In the theoretical model[2] the excitonic wave function was written as a product of the T-wire eigenstates for the electron and hole and a variational wave function for the e-h correlated state. A trial wave function that better reproduced the experimental data was shown to be that in which the e-h correlation was in all three directions. In the work of Goldini *et al.*,[3] a detailed study of the spin mixing in the valence band, neglecting the e-h Coulomb interaction, has shown that the character of the hole state (as being heavy or light) depends on the degree of the wave function spreading over the arm and stem quantum wells. This has an important effect on the optical anisotropy for excitation with linear polarization parallel or perpendicular to the wire axis. A bias with an electric field perpendicular to the wire can be used to control the e-h wave-function overlap in the system and therefore to modulate the polarization-dependent absorption, allowing for the development of polarization-sensitive detectors, modulators, and filters, as suggested by Citrin and Chang.[4]

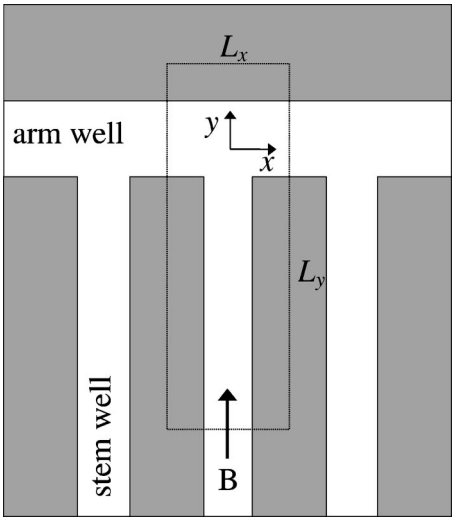

FIG. 1. Illustration of the T-wire system periodic in the x direction. In dotted lines is the unit cell region used in the numerical calculation.

The optical-absorption spectrum of a cylindrical quantum wire was recently calculated by Hughes and Citrin,[5] who solved the low-density semiconductor Bloch equation (SBE) in the time and real-space domains. The time evolution of the interband optical polarization was obtained by wave-packet propagation implemented by split-step method in which the action of the kinetic operator is carried out in the Fourier space and transformed back to real space, while the action of the potential term is carried out directly in real space. A complete approach in real-space treats the kinetic-energy operator for the *e-h* relative coordinates as a second-order derivative with respect to these coordinates. The optical spectrum was obtained by Fourier transforming the time-dependent *e-h* polarization to the frequency domain. From the peaks in the spectral response one can find the eigenenergies of the *e-h* pair in the wire without having to rely on restrictive basis expansion, perturbation, or variational methods. Using the full SBE,[6] i.e., including nonlinear contributions, the spectral calculation yields at once the *e-h* bound states as well as the continuum of the free *e-h* pairs depending on the photocarrier density, which is important to the understanding of the exciton stability and band-gap renormalization in wire systems under high excitation power (see, for example, Refs. 7–9). Even in the low-density limit, this method is also handy to calculate optical absorption of systems having potentials that are time dependent[10] or having no true *e-h* bound state, such as in the case when an intense static electric field is applied along the quantum wire.[5] The absorption spectra in the presence of such static field shows interesting characteristics (Franz-Keldysh effect[11]) such as energy shifts, oscillations in the continuum part of the spectra,[12] and a broadening of the fundamental transition indicating the *e-h* bound state has become unstable, i.e., its lifetime is reduced. However, the presence of this static electric field breaks the translational invariance along the wire and the periodic boundary condition fails. Consequently, in order to avoid spurious boundary effects on the wire, we shall not treat the kinetic operator in Fourier space, as done in Ref. 5.

In this work we study the electroabsorption of magnetoexcitons in a T-shaped quantum wire, where the magnetic field is applied perpendicularly to the plane of the arm well and an electric field is applied along the wire axis. The excitonic energies are calculated from the absorption spectra as in Ref. 5 but with the kinetic operator in the real-space representation, avoiding in this way the failed periodic boundary condition. The peak and the linewidth of the optical absorption for the fundamental transition are investigated as functions of the strength of both fields, magnetic and electric. The optical spectra are obtained using an effective 1D potential for the Coulomb attraction of the *e-h* pair, which was calculated using the electron and hole ground states for the laterally confined carriers in a T-wire structure. These states are calculated numerically by solving the 2D Schrödinger equation.

I. OPTICAL ABSORPTION OF A T-SHAPED SEMICONDUCTOR QUANTUM WIRE

A. Electron and hole lateral states

We begin formulating the problem of an electron and a hole in a T-wire structure as in Fig. 1. In this section we do not consider *e-h* interaction. The ground states we calculate are needed in the next section to construct the *e-h* interaction potential used in the calculation of the optical-absorption spectrum of the wire.

We first consider the Schrödinger equation for an electron in the wire,

$$H^e_{2D}\phi^e_n=\left[\frac{1}{2m_e}\left(\mathbf{p}_e-\frac{q_e}{c}\mathbf{A}\right)^2+V^e_{2D}\right]\phi^e_n=E^e_n\phi^e_n, \qquad (1)$$

where m_e is the effective mass, q_e the electron charge, $\mathbf{p}_e=-i\hbar\nabla_e$, and V^e_{2D} describes the T-wire potential due to material bandgap differences. This potential is a function of the lateral coordinates of the system cross section (xy plane) as in Fig. 1. Unit cells of sizes L_x and L_y were used with periodic boundary conditions along the x direction and hard walls for the boundaries in the y direction. For a magnetic field perpendicular to the plane of the arm well we used a gauge which preserves the translational invariance along the wire, namely

$$\mathbf{A}=\mathbf{A}(\mathbf{r}_e)=-Bx_e\hat{\mathbf{z}}. \qquad (2)$$

Then the kinetic-energy term can be written as

$$\frac{1}{2m_e}\left(\mathbf{p}_e-\frac{q_e}{c}\mathbf{A}\right)^2=\frac{\mathbf{p}_e^2}{2m_e}-\frac{q_eBx_ep_{ez}}{m_ec}+\frac{q_e^2B^2x_e^2}{2m_ec^2}. \qquad (3)$$

Equations similar to Eqs. (1)–(3) were obtained for the heavy holes. Parabolic energy dispersions for the heavy holes were considered with anisotropic effective masses $m_{hx}=m_{hz}$ and m_{hy}. This approximation ignores the strong state mixing for holes having nonzero momenta and/or at excited subband states.[3,13] For states close to the band edge this approximation is satisfactory, but polarization effects are then neglected.

The second term on the right-hand side (rhs) of Eq. (3) couples the carrier free motion along the wire (z axis) with the confined motion in the xy plane of the wire. Treating this coupling together with the *e-h* Coulomb interaction is a difficult task. The *e-h* interaction is included in our model when calculating the optical-absorption spectrum (see Sec. I B). Then a pulse of light creates *e-h* pairs having zero center-of-mass momentum. The correlation of the *e-h* relative motion results in momentum distributions for the electrons and holes around the zero momentum, $k_z=0$. In this case, the neglect of the second term on the rhs of Eq. (3) is satisfactory. The last term on the rhs of Eq. (3) favors the confinement of the electrons and holes around the wire for a nonzero B field, yielding energy shifts of the electron and hole subbands. The 2D Schrödinger equations for electrons and holes, as just defined, are then solved numerically, using the same technique as in Ref. 14, for the ground-state wave functions $\phi^e_0(x_e,y_e)$ and $\phi^h_0(x_h,y_h)$.

B. Optical absorption

The optical absorption is calculated from the interband polarization whose equation of motion is given by the SBE. We consider an optical pulse exciting states around the band

gap, such that only the lowest conduction and highest valence subbands of the wire participate. Coulomb interaction between the electron and hole is then included. For that, an effective potential is calculated using the ground-state wave functions obtained as in Sec. I A, that is

$$V(z) = -e^2 \int d^2\rho_e \int d^2\rho_h \frac{|\phi_0^e(\rho_e)|^2 |\phi_0^h(\rho_h)|^2}{\sqrt{z^2 + (\rho_e - \rho_h)^2}}, \quad (4)$$

where z is the e-h relative coordinate along the wire axis. Therefore, the problem has been reduced to one direction.

In the real-space representation, the SBE's, in the limit of low excitation read[6,5]

$$i\hbar(\partial_t + i\omega_g + \Gamma)P(z,t) = HP(z,t) + d_{cv}E(t) \times [2n(z,t) - L\delta(z)], \quad (5)$$

$$i\hbar\partial_t n(z,t) = -d_{cv}E(t)P^*(-z,t) + d_{cv}^* E^*(t)P(z,t), \quad (6)$$

where

$$H = -\frac{\hbar^2}{2\mu}\frac{\partial^2}{\partial z^2} + V(z) + eFz, \quad (7)$$

with L being the wire length, $z = z_h - z_e$ the e-h relative coordinate along the wire, F an applied longitudinal electric field, μ the e-h reduced mass ($\mu^{-1} = m_e^{-1} + m_{hz}^{-1}$), d_{cv} the interband dipole moment, $\hbar\omega_g$ the band-gap energy (or better, the onset of the continuum of free states in the wire) and $E(t)$ the optical pulse. The relaxation rate Γ, accounting for scattering processes causing dephasing of the optical polarization, is treated within the relaxation time approximation.

Equations (5) and (6) describe the space-time evolution of the interband optical polarization $P(z,t)$ and the carrier occupation $n(z,t)$. The effect of this occupation is to bleach the absorption due to phase-space filling. We have not included in the present calculation nonlinear terms in Eqs. (5) and (6) responsible for band-gap renormalization and vertex and local-field corrections. These terms are important when treating high-density, or high excitation situations.[6]

The optical absorption is calculated from the interband polarization according to[6]

$$\alpha(\omega) = \sqrt{\mu_{bg}} \frac{\omega\varepsilon''(\omega)}{\sqrt{\frac{1}{2}[\varepsilon'(\omega) + \sqrt{(\varepsilon'(\omega))^2 + (\varepsilon''(\omega))^2}]}}, \quad (8)$$

where μ_{bg} is the background permissivity,

$$\varepsilon'(\omega) = \varepsilon_{bg} + \mathrm{Re}[\chi(\omega)], \quad \varepsilon''(\omega) = \mathrm{Im}[\chi(\omega)], \quad (9)$$

$$\chi(\omega) = \frac{P(\omega)}{VE(\omega)}, \quad (10)$$

where V is the system volume, with $P(\omega)$ and $E(\omega)$ being the Fourier transforms of the interband polarization $P(t) = d_{cv}P(x=0,t) + \text{c.c.}$ and of the optical pulse $E(t)$, respectively.

The time-dependent solutions of Eqs. (5) and (6) are implemented as shown in the Appendix. The kinetic-energy derivative is carried out in real space, which for the discretized wire length requires the solution of a linear system of equations involving a tridiagonal matrix by Gauss elimination. Our time propagation scheme is correct up to second order in the time interval, i.e. up to Δt^2. To include the nonlinear terms in the SBE, which were neglected in Eqs. (5) and (6), one has to propagate the solutions at least up to Δt^3. The Fourier transforms $P(\omega)$ and $E(\omega)$ were obtained using fast Fourier transform algorithm.

II. RESULTS AND DISCUSSION

We have investigated a T-wire system made of $GaAs/Al_{0.3}Ga_{0.7}As$ semiconductors for which the effective masses are $m_e = 0.067m_0$ for an electron and $m_{hx} = m_{hz} = 0.13m_0$ and $m_{hy} = 0.34m_0$ for a heavy hole, with m_0 being the free-electron mass. The effective masses are considered to be the same for the well and barrier materials. The potential barriers, due to the band-gap energy difference of such materials, are $V^e = 219.7$ meV for the conduction electron and for the valence heavy hole $V^h = 134.6$ meV. The dielectric constant used is $\varepsilon_{bg} = 13.1\varepsilon_0$, and the interband dipole moment is $d_{cv} = 3$ eÅ. The system investigated is similar to a T wire previously studied experimentally[1] and theoretically.[2] It has an arm quantum well of width 5.6 nm and a stem quantum well of width 5.1 nm. Unit cells representing the system (Fig. 1), of sizes $L_x = 120$ nm and $L_y = 40$ nm, was used in the calculation of the lateral states with the respective numbers of points in the mesh $N_x = 256$ and $N_y = 161$. For the same system studied in Refs. 1 and 2 (named sample S3) we verified that the wire ground states had appreciable wave function penetration into neighboring unit cells. To avoid that, and to guarantee truly quasi-1D states, we have used a somewhat larger unit cell along the x direction. In Fig. 2 are the wave function projections for an electron in zero magnetic field and in $B = 8$ T. One can see that the effect of the field is to enhance the electron confinement into the wire. We were careful in not using too high values of B for which the wave functions would spread considerably over the stem well requiring caution with the use of our boundary conditions along the y direction. A similar behavior was observed for the heavy-hole ground state.

In Fig. 3(a) we plot (open triangles) the electron-hole energy transition (without Coulomb interaction) as a function of the applied magnetic field. This energy comprises the zero-point energies of the electron and hole in the wire, obtained as in Sec. I A, plus the bandgap energy ($E_{gap} = 1519$ meV for GaAs). This curve yields the onset of the wire continuum. When the Coulomb interaction is turned on, the exciton energy is calculated from the peak in optical absorption spectrum as discussed in Sec. I B.[15] The inset in Fig. 3(a) shows some of these spectra; those with broader peaks are calculated using an inverse dephasing rate $\Gamma^{-1} = 500$ fs, for $B = 0$ and 8 T, and the spectrum with a narrower peak is calculated with $\Gamma^{-1} = 1000$ fs, for $B = 0$. In the latter spectrum one can see, besides the fundamental exciton transition, a small peak close to the continuum onset

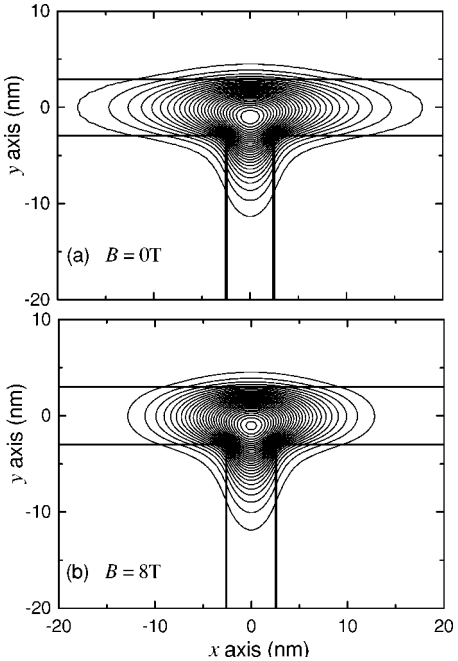

FIG. 2. (a) Projection of the ground-state wave function for an electron in the T wire in the absence of an applied magnetic field $B=0$. (b) Same as before but for $B=8$ T.

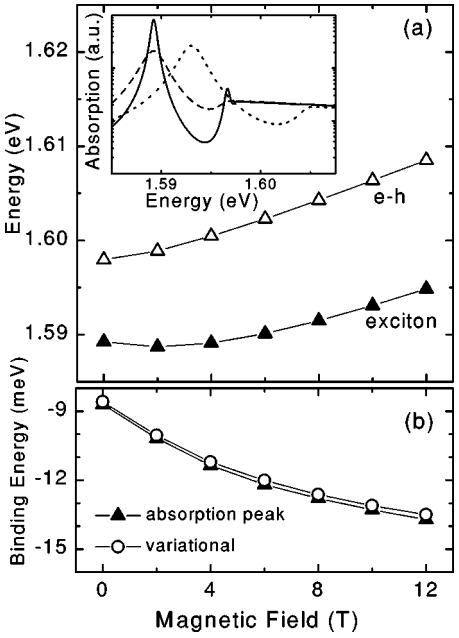

FIG. 3. (a) Electron-hole transition energy (e-h) and exciton fundamental transition energy as functions of the applied magnetic field. The inset shows the optical absorption spectra for an inverse dephasing rate $\Gamma^{-1}=500$ fs, for $B=0$ (dashed line) and $B=8$ T (dotted line). The solid line is for $\Gamma^{-1}=1000$ fs and $B=0$. (b) Exciton energy in relation to the wire continuum as a function of the magnetic field from a variational method calculation and from the energy position of the absorption fundamental peak.

due to excited excitonic transitions. In Fig. 3(a) the fundamental exciton peak positions are plotted (solid triangle) for different applied magnetic fields. A blueshift of the peak can be observed in qualitative agreement with the experiment.[1] The apparent overestimation to blueshift of our result, when one compares it quantitatively with the experimental data or with the results from other model calculation,[2] is due to the fact we have used a larger system to ensure that our spectral calculation could be applied to a truly 1D system without wave-function penetration into neighboring unit cells. We compare also our results with that one obtained performing a variational calculation using the same Coulomb potential generated as in Eq. (4). The trial wave function used—$\psi(z)=A\exp(-az^2)$, where a is the variational parameter—has e-h correlation only for the coordinates along the wire. In Fig. 3(b) we show the binding energy, i.e. the difference in energy from the e-h bound state to the continuum onset shown in Fig. 3(a), calculated from the variational method and from the optical absorption peaks [Fig. 3(a)]. As expected the binding energy from the variational method is slightly smaller than the result extracted from the absorption peaks. We also see in Fig. 3(b) that, although a blueshift is seen in Fig. 3(a), the magnetoexciton binding energy is enhanced with increasing applied magnetic field due to the forced proximity of the electron and hole in the wire.

The advantage of using the optical absorption method over the variational calculation is in the fact it can also be applied to systems with effective e-h potentials without true bound states and to systems subject to time-dependent potentials. In the following we present a study that exemplifies this point. For a static electric field applied along the wire axis, the electron and hole in the exciton is pulled apart by the field which introduces an additional potential eFz to the effective Coulomb potential $V(z)$ [note that $V(z)$ does not diverge at $z=0$ for quasi-1D systems[6]]. The total potential is now approximately linear at large z, with no minimum at $z=0$, which makes the attempts of finding e-h bound states around $z=0$ via variational and perturbative methods for large fields F unfruitful, while the solution using the optical absorption is still easily realized. In Fig. 4(b) we show the absorption spectra for the same T wire as investigated before, with $B=4$ T for $F=0$ (dotted line) and $F=4.5$ kV/cm (solid line). One sees that the effects of the longitudinal electric field are (i) to broaden the fundamental exciton peak, (ii) to shift the peak, and (iii) to produce oscillations in the continuum part of the spectrum. Here we focus our attention on the fundamental exciton transition. In Fig. 4(a) we plot the absorption peak, relative to the continuum onset, for different applied magnetic fields as a function of the electric field. The binding energy enhances slightly and then recovers as the electric field is increased. The approximate constancy of the fundamental excitonic state was already predicted long ago in 2D (Ref. 16) and 3D (Ref. 17) systems and observed in quantum wells,[18] where the main effect seen was the broadening of the exciton fundamental optical transition.

We note, from Fig. 4(c), that the broadening of the fundamental line is more pronounced for magnetoexcitons subject to lower magnetic field. The linewidth broadening is related to the reduction of the lifetime of the exciton state, which becomes unstable due to the electric field. Figure 4(d)

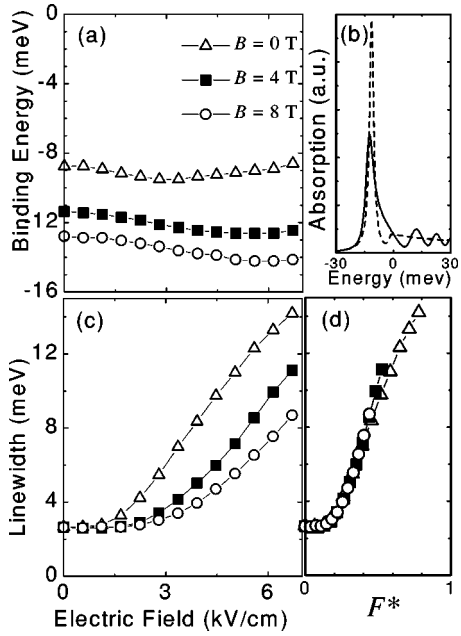

FIG. 4. (a) Magnetoexciton binding energies as functions of the longitudinal electric field. (b) Optical absorption spectra for $B=4$ T, without (dashed line) and with an applied longitudinal electric field $F=4.5$ kV/cm (solid line). (c) Linewidths (full width at half maximum) of the fundamental exciton absorption for different magnetic fields as functions of the electric field. (d) The same as in (c) but with the horizontal axis being a scaled electric field.

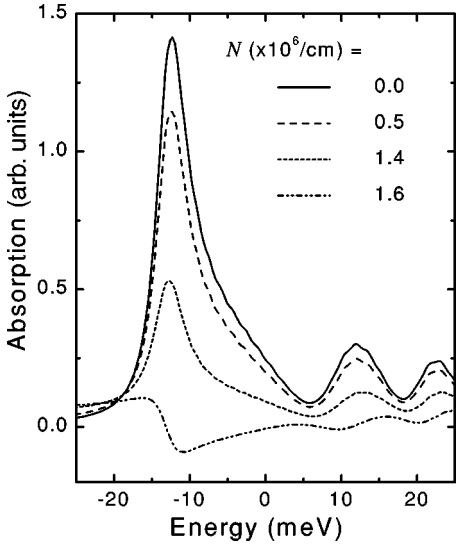

FIG. 5. Optical absorption spectra for different intensities of the exciting light creating excitonic densities shown at the legend.

shows that the different curves in Fig. 4(c) become essential only when they are plotted as a function of a conveniently scaled electric field F^*. It is given by $F^* \sim e a_0 F/E_B$, where a_0 and E_B are, respectively, the exciton effective Bohr radius and the binding energy, which are calculated in absence of an electrical field, $F=0$. The value $F^* \sim 1$ is related to the field necessary to ionize the exciton.

So far the bleaching effect due to the carrier occupation has not been included in the SBE; i.e. Eq. (5) was treated with $n(z,t)=0$. We now solve Eqs. (5) and (6) together. In this case, the absorption depends on the intensity of the optical pulse E_0. In Fig. 5 we show the absorption spectra calculated for the magnetoexciton with $B=4$ T in an applied electric field $F=4.5$ kV/cm for different values of the optical pulse intensity E_0. This results in different photoexcited carrier concentrations N, which can be obtained in our model from $n(z,t)$ calculated at $z=0$ and $t \gg \Gamma^{-1}$ since Eq. (6) has no damping and $n(z=0)=\Sigma_k n_k \equiv N/2$, where n_k is the occupation in k space and the factor 2 accounts for the spins (note that the twofold spin channels $\sigma^{\pm}$ are independent in this model). As the time duration of the exciting pulse is short, 40 fs, it has a very broad spectral band that excites carriers within a large energy band. Due to phase-space filling, we then observe a bleaching of the absorption uniformly over the energy range investigated. A negative absorption is observed in the case of strong pump where N is larger than $\sim 1.5 \times 10^6$/cm. This is in the order of N for which the Mott transition (i.e., the merge of the exciton peak at the e-h continuum) is expected,[8,9] and optical gain has being observed in real quantum wires.[7]

In conclusion, we have investigated the magnetoexciton fundamental state in a T-shaped semiconductor quantum wire. The e-h effective potential was calculated from the ground-state wave functions for the electron and hole in the wire obtained by solving the 2D Schrödinger equation numerically. The optical-absorption spectrum was used to extract the energy and the linewidth of the fundamental magnetoexciton state. An enhancement of the exciton binding energy with increasing magnetic field was observed[2] and, as in the experiment,[1] a blueshift of the fundamental transition was calculated. A study of the magnetoexciton in the T wire in an applied electric field has shown that the energy position of the fundamental transition is weakly affected by the electric field. Its linewidth broadens in a way that can be scaled by the exciton binding energy and the Bohr radius. It is worth mention that although we have investigated a unidimensional model, for which the lateral and longitudinal degrees of freedom of the carrier motion in the wire were separated, there is in principle no limitation to implement the method to solve the SBE in three full dimensions, even including nonlinear terms.

Finally, in comparing our results to the experimental data one has to consider exciton localization in imperfections of the quantum wires. This yields an inhomogeneous broadening of the emission peaks with linewidths of order of $\Gamma_i \sim 3-10$ meV, although sharp spectral structures in the photoluminescence spectrum have been observed and attributed[9] to individual localized-exciton recombinations. A similar broadening of the absorption peak may occur for photoexcitation of excitons in different regions of the quantum wire. We believe our results, i.e., the dependence of the energy shifts and linewidths on the magnetic and electric fields (cf. Figs. 3 and 4), can be experimentally observed since they are of the same order or larger than Γ_i.

ACKNOWLEDGMENT

We acknowledge support from FAPESP (Brazil).

APPENDIX: SOLUTION OF SBE

We consider the light pulse tuned at the gap frequency, i.e., $E(t)=e^{-i\omega_g t}f(t)$, where $f(t)$ is a gaussian envelope with width σ at e^{-2} of its maximum. In order to perform the solution of the system of equations (5) and (6) we make the follow changes of scale:

$$\overline{P}(z,t)=\frac{\hbar}{E_0 d_{cv}\Delta t}e^{-i\omega_g t}P(z,t) \tag{A1}$$

and

$$\overline{n}(z,t)=\frac{1}{2}\left(\frac{\hbar}{E_0 d_{cv}\Delta t}\right)^2 n(z,t), \tag{A2}$$

which let the system of equations independent on the gap energy and makes explicit its dependence on Δt. The solution of the SBE for these scaled variables $\overline{P}$ and $\overline{n}$ is given by

$$\overline{P}(z,t_{j+1})=e^{-\Gamma\Delta t}\exp\left\{\frac{\Delta t}{i\hbar}H(z,t_j)\right\}\left\{\overline{P}(z,t_j)+if(t_j)\times\left[L\,\delta(z)-\left(\frac{2E_0 d_{cv}\Delta t}{\hbar}\right)^2\overline{n}(z,t_j)\right]\right\}, \tag{A3}$$

with the initial conditions $\overline{P}(z,t_0)=\overline{n}(z,t_0)=0$. The nonlinear terms, the renormalization gap, and the local-field correction, missing in Eqs. (5) and (6), would contribute to the solution above with terms proportional to Δt^3. As we have neglected them (low excitation regime) and kept only terms up to Δt^2, we perform the time evolution operator (exponential of the Hamiltonian H) using the split-step method up to second order in Δt, when it is applied to the first two terms on the rhs of Eq. (A3), $\overline{P}(z,t_j)$ and $if(t_j)L\,\delta(z)$, and approximate it up to zero order, i.e., $\exp\{(\Delta t/i\hbar)H(z,t_j)\}\simeq 1$, when it is applied to the last term, namely, the population $\overline{n}(z,t_j)$, because it is already proportional to Δt^2.

[1] T. Someya, H. Akiyama, and H. Sakaki, Phys. Rev. Lett. **74**, 3664 (1995).

[2] G. W. Bryant and Y. B. Band, Phys. Rev. B **63**, 115304 (2001).

[3] G. Goldoni, F. Rossi, E. Molinari, and A. Fasolino, Phys. Rev. B **55**, 7110 (1997).

[4] D. S. Citrin and Y.-C. Chang, Appl. Phys. Lett. **59**, 582 (1991).

[5] S. Hughes and D. S. Citrin, Phys. Rev. Lett. **84**, 4228 (2000).

[6] H. Haug and S. W. Koch, *Quantum Theory of the Optical and Electronic Properties of Semiconductors*, 3rd ed. (World Scientific, Singapore, 1994).

[7] W. Wegscheider, L. N. Pfeiffer, M. M. Dignam, A. Pinczuk, K. W. West, S. L. McCall, and R. Hull, Phys. Rev. Lett. **71**, 4071 (1993).

[8] S. Das Sarma and D. W. Wang, Phys. Rev. Lett. **84**, 2010 (2002).

[9] S. Sedlmaier, M. Stopa, G. Schedelbeck, W. Wegscheider, and G. Abstreiter, Phys. Rev. B **65**, 201304 (2002).

[10] S. Hughes, Phys. Rev. B **63**, 153308 (2001).

[11] W. Franz, in *Tunneling Phenomena in Solids*, edited by E. Burstein and S. Lundqvist (Plenum Press, New York, 1969), Chap. 15.

[12] J. Callaway, Phys. Rev. **130**, 549 (1963).

[13] D. S. Citrin and Y.-C. Chang, Phys. Rev. B **43**, 11 703 (1991).

[14] M. H. Degani, Appl. Phys. Lett. **59**, 57 (1991); M. H. Degani and J. P. Leburton, Phys. Rev. B **44**, 10 901 (1991).

[15] To solve the spatial and time-dependent equations (5) and (6) we discretized the relative *e-h* distance in intervals of 1 Å using 30000 points. Time was discretized in intervals of 1.5 fs with a total of 2^{15} points used [for Fig. 5 we had to use 0.2 fs and 2 (Ref. 18), respectively, to correctly obtain $n(z,t)$]. The optical pulse exciting the wire was assumed to be a Gaussian of full width $\sigma=40$ fs, with spectral weight centered at the continuum onset for $B=0$ and $F=0$ (i.e., $\hbar\omega=1598$ meV).

[16] F. L. Lederman and J. D. Dow, Phys. Rev. **13**, 1633 (1976).

[17] J. D. Dow and D. Redfield, Phys. Rev. B **1**, 3358 (1970).

[18] D. A. B. Miller, D. S. Chemla, T. C. Damen, A. C. Gossard, W. Wiegmann, T. H. Wood, and C. A. Burrus, Phys. Rev. B **32**, 1043 (1985).